Advances in Science and Technology Research Journal

Advances in Science and Technology Research Journal 2024, 18(2), 266–283
https://doi.org/10.12913/22998624/184339
ISSN 2299-8624, License CC-BY 4.0

Received: 2023.11.20
Accepted: 2024.02.20
Published: 2024.03.15

Shaping the Topography of the Active Surface of a Ceramic Grinding Wheel with a Stationary Multi-Point Diamond Dresser

Ryszard Dębkowski[1*], Marcin Gołąbczak[1]

[1] Institute of Machine Tools and Production Engineering, Faculty of Mechanical Engineering, Lodz University of Technology, ul. Stefanowskiego 1/15 0, 90-537 Łódź, Poland

* Corresponding author's e-mail: ryszard.debkowski@p.lodz.pl

ABSTRACT

Stationary multi-point diamond dressers are an economical alternative to single-point dressers. However, when using them, it is necessary to keep in mind the different way of shaping the surface topography of the wheel being dressed. During one dressing pass, the grinding wheel is affected by several diamonds fixed at specific distances on the dresser surface. The simulation studies presented in the paper showed that, depending on the dressing feed and the distance and active width of the diamonds, the overlap of their motion paths is not the same over the entire grinding wheel surface, as is the case when single-point dressers are used - the grinding wheel surface consists of areas shaped with different overlap ratios. Taking into account the results of simulation studies, formulas were proposed for calculating two new indicators to supervise the dressing process with stationary multi-point dressers. Experimental dressing tests using new indicators and the evaluation of the vitrified grinding wheel topography confirmed the usefulness of using the new indicators and the inhomogeneity of the grinding wheel surface topography, resulting from the different overlapping of the motion paths of individual dresser diamonds.

Keywords: dressing, dressing indicator, grinding wheel, overlap ratio, grinding wheel topography, multi-point diamond dresser.

INTRODUCTION

The topography of the grinding wheel active surface specified by the shape, size, and distribution of abrasive grain edges in the working space, plays a crucial role in the grinding process. The grinding process and the machining outcome depend on its condition. The topography of a grinding wheel's active surface, prepared for operation, is the result of the grinding wheel's characteristics (i.e., size and type of abrasive grains and wheel structure) and the dressing operation carried out.

Machine dressing of conventional grinding wheels with aluminum oxide or silicon carbide abrasives is generally carried out using diamond dressers. This group includes, among others, stationary single and multi-point dressers and roller dressers (Fig. 1). Natural or synthetic diamonds in the form of mono- or polycrystalline are used in the construction of dressers. Arrangement of diamond crystals or PVD, CVD, MCD needles on the dresser surface can be random or defined [1, 2]. In the case of single-point dressers the diamond is in the axis of the dresser (Fig. 1a). In the case of stationary multi-point dressers, similarly to the needles in PVD, CVD, MVD dressers, diamonds are in a specific position in relation to each other (Fig. 1b, c), and in roller dressers diamonds can be arranged both in a defined and random way (Fig. 1d). Dressing parameters, determining the relative motion of the dressing tool and grinding wheel, have a significant impact on the obtained grinding wheel surface topography. By changing the values of these parameters, the cutting properties of the grinding wheel can be influenced in a targeted manner, and consequently the course and the achieved grinding result. For stationary dressers, these parameters are the dressing depth a_d and the dressing feed f_d and

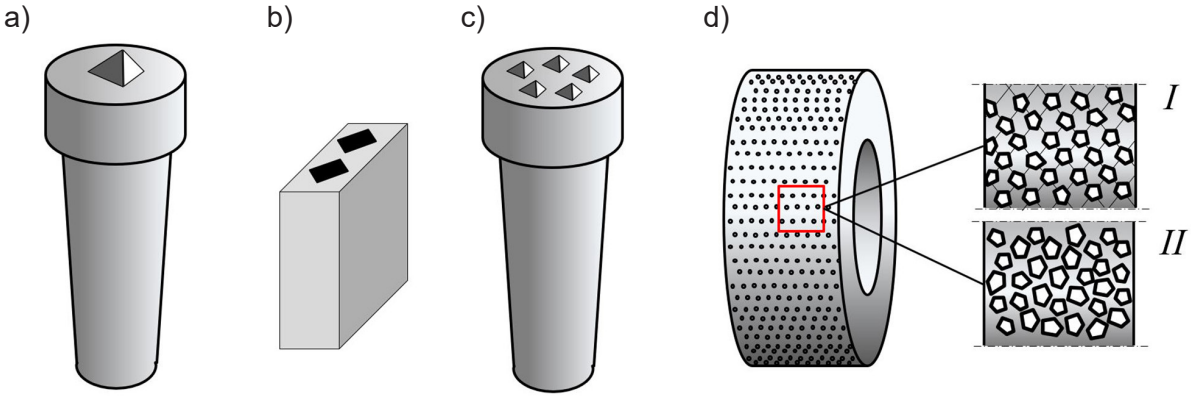

Figure 1. Diamond dressers – examples: (a) single-point dresser, (b) needle blade dresser, (c) stationary multi-point dresser, (d) roller dresser: I – defined distribution of diamond grits, II – random distribution of diamond grits

for roller dressers, the radial infeed speed v_{fd} and the direction and values of the peripheral speeds of the grinding wheel v_{sd} and of the dressing tool v_d. The aforementioned parameters are included in the indicators that characterize the dressing process [1, 3]. The basic ratio, which is mainly used in dressing processes performed with the use of diamond single-point dressers, is the overlap ratio U_d – Equation 1. Its formula takes into account the dressing feed f_d and the active width of the diamond tip measured in the direction of the dressing feed b_d. The result of calculations according to the Equation 1 indicates how many revolutions the grinding wheel will make during the movement of the dressing tool on a section equal to the active width of the diamond.

$$U_d = \frac{b_d}{f_d} \text{ or } U_d = \frac{b_d \cdot n_s}{v_{fdr}} \quad (1)$$

where: b_d – active width of the diamond tip [mm], f_d – dressing feed [mm/rev], n_s – rotational speed of the grinding wheel [1/s], v_{fdr} – dresser feed rate [mm/s].

When using roller dressers to control dressing conditions, the ratio q_d is applied, which describes the relative motion of the wheel and the dresser. The ratio q_d determines what fraction of the circumferential speed of the grinding wheel v_{sd} is the dressing speed v_d – Equation 2. The ratio takes a positive value when the rotations of the dresser and grinding wheel are synchronous and negative when they are asynchronous.

$$q_d = \frac{v_d}{v_{sd}} \quad (2)$$

where: v_d – circumferential speed of the dresser [m/s], v_{sd} – circumferential speed of the grinding wheel [m/s].

Another, more complex index i_d – Equation 3, determining the number of collisions between the dresser diamonds and CBN grains, was used to characterize the dressing operation with a diamond cup dresser of CBN ceramic grinding wheels [4]. This index combines the kinematic conditions of the dressing process, defined by the U_d, q_d indexes, and the characteristic data of the dressing tool and the grinding wheel.

$$i_d = C'_{K,Dt} \cdot l_{gd} \cdot (D_{CBN} + D_{Dt}) \cdot U_d \cdot |1 - q_d| \quad (3)$$

where: l_{gd} – geometric contact length [mm], $C'_{K,Dt}$ – density of diamond dresser grains [mm^{-2}], D_{CBN} – average CBN grain size [mm], D_{Dt} – average diamond grain size [mm], U_d – overlap ratio [–], q_d – speed ratio [–].

The values of the listed indicators and the parameter specifying the depth of dressing (per revolution or per pass) make it possible to supervise the dressing process and predict the obtained topography of the grinding wheel. As indicated in [4–6], the final topography of the grinding wheel is significantly influenced by the collisions number of diamonds with grinding wheel abrasive grains. In the case of using stationary dressers, the increase in the collisions number is achieved by increasing the value of the U_d ratio. The higher the number of collisions, the lower the roughness of the grinding wheel topography after dressing [6].

Number of collisions when using rotating diamond cup dresser for dressing vitrified CBN grinding wheels [4, 5] is a function of the overlap ratio U_d and the relative dressing speed. According to [4], high collision numbers together with high effective dressing speeds cause intensified CBN grits splintering, while small collision numbers

and reduced effective dressing speeds result mostly in grits flattening. In turn, the authors [5] indicate that the use of a high value of the q_d ratio is recommended for roughing the grinding wheel surface, during which a larger number of cutting edges is created.

The topography of grinding wheels dressed with diamond roller dressers depends mainly on the value of the q_d ratio and the radial feed v_{fd} [1, 3, 7]. The influence of the q_g ratio (diamond roller dresser grit size / grinding wheel grit size) and the type of diamonds used in the dresser are also considered [8]. A smaller active surface roughness of the grinding wheels is obtained by limiting the infeed speed (then the dressing depth a_d will be reduced) and increasing the relative speed of the dressing wheel and grinding wheel (using the asynchronous movement of the grinding wheel and the dresser) [1, 3, 6, 7, 8]. A typical graph of the dependence of the active roughness of the grinding wheel on the dressing conditions is shown in Figure 2a [1–3]. Depending on the direction of rotation of the dresser and the grinding wheel, the shape of contact paths between the diamond grains of the dressing wheel and the grinding wheel changes. During up-dressing, the paths are longer, so that the microgeometry produced on the grinding wheel is characterized by a lower roughness in relation to the roughness after down-dressing, in which the contact paths are shorter and more curved. A special case occurs when the grinding wheel and dresser synchronous move at the same circumferential speeds (q_d= 1). The grinding wheel surface is crushed by diamond grits, as a result of which the surface of the grinding wheel obtains the highest roughness. Studies of the influence of dressing conditions with single-point dressing tools [1, 3, 4, 9, 10, 11, 12] on the grinding wheel topography indicate that decreasing the U_d ratio and/or increasing dressing depth a_d results in a greater roughness of the grinding wheel (Fig. 2b) and a smaller number of static cutting edges distributed at a greater depth [9, 10, 13], which translates into lower values of the forces of the grinding process [14]. When the ratio takes values below 1, a helical groove is formed on the grinding wheel surface - unacceptable during the finishing machining of workpieces, but useful when the purpose of grinding is a surface with a specific microstructure pattern [15].

When using stationary multi-point diamond dressers, e.g. diamond sticks, the factor affecting the final topography of the wheel is incomplete removal of the wheel layer during one dressing pass [16]. This leads to the accumulation of the thickness of the removed layer in the next dressing pass and, consequently, to greater contact loads and greater roughness of the grinding wheel. The source of this phenomenon is the random nature of the diamonds grains distribution in the dressing tool and the irregular shape of these grains.

As the literature review shows, the condition of the topography of the grinding wheel active surface can be shaped by changing the parameters of the dressing method used. A convenient tool to help predict the effects of dressing are the dressing indicators discussed above. Their values, calculated on the basis of formulas containing characteristic values of a given dressing process, indicate what active roughness of the grinding wheel should be expected after dressing. Unfortunately, these indicators are not applicable to dressing operations performed with stationary multi-point dressers - they do not take into account the

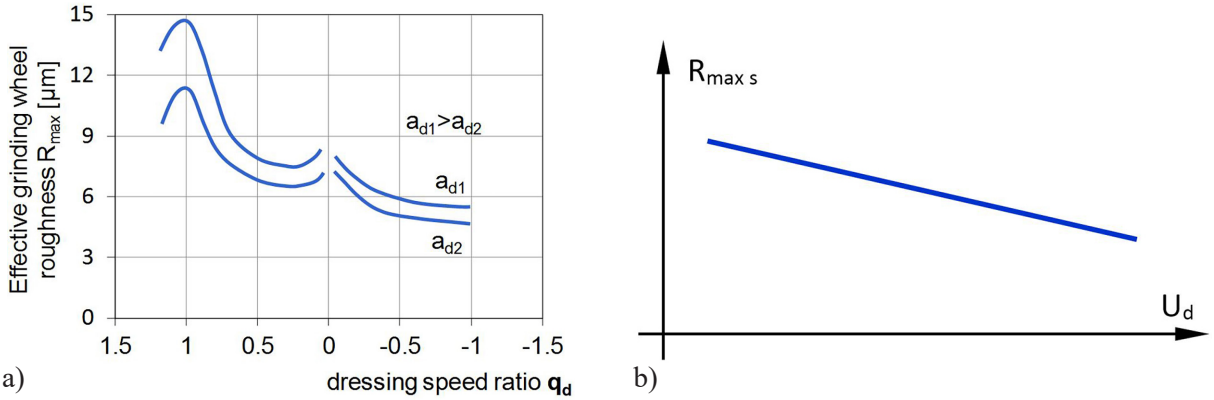

Figure 2. Influence of dressing parameters on the effective grinding wheel roughness: (a) roller dresser, (b) single-point dresser (own figure based on [28])

specificity of shaping the topography of the grinding wheel surface by several diamonds placed on the dresser surface. These diamonds, during the dressing pass, come into contact with the surface of the grinding wheel one by one and move in tracks that may overlap to varying degrees depending on the dressing feed. In order to develop new formulas of indicators useful for this dressing method, research was undertaken to explain how the kinematic parameters of dressing and the condition, number and position of diamond grains of a stationary multi-point dresser affect the method of removing the grinding wheel layer and, consequently, the topography of its surface.

This research was divided into two stages. In the first one, the results of which were to be used to develop new dressing indicators, simulation study of the overlapping of diamond grain paths along the grinding wheel generatrix were carried out. In the second stage, experimental tests were carried out in which, using new indicators, a series of tests were performed on dressing the grinding wheel using a stationary multi-point dresser, and then measuring and assessing the topography of the grinding wheel dressed in this way.

Characteristics of dressing with stationary multi-point diamond dresser

On the working surface of stationary multi-point dressers (Fig. 1c) there is a specific number of regularly distributed diamonds grits. The distances between the diamonds cause that during dressing the contact of subsequent diamonds with the surface of a rotating grinding wheel occurs in different angular its position. Depending on the dressing feed and the number and distance of the diamonds, the paths created by the diamonds may overlap to varying degrees. Figure 3 shows an example of how the traces of diamonds movement paths created on the grinding wheel generatrix during one dressing pass are superimposed. Five colors indicate the position of the dresser diamonds in five consecutive revolutions of the grinding wheel for two different dressing feed rates f_d. When drawing the diagrams, it was assumed that the distances l between the diamonds of the dresser, measured in the direction of feed, are the same.

In both presented on the Figure 3 cases, the dressing feed f_d, counted per one revolution of the grinding wheel, is not a multiple of the diamond distance ($f_d \neq n \cdot l$). So we are not dealing with a special situation when successive diamonds move along the paths of their predecessors. As can be seen, on the grinding wheel generatrix there are sections with different multiplicity of contact with the diamond tips and sections that did not have this contact at all. As a result, spiral microbands will be formed on the grinding wheel surface, which, as follows from Figure 2b, will have different roughness. Whereas the areas that did not come into contact with the dresser will form a helical ridge on the surface of the grinding wheel. Thus, the grinding wheel surface formed with the stationary multi-point diamond dresser does not have a homogeneous structure. Its condition depends on the geometrical characteristics of the diamonds, their mutual

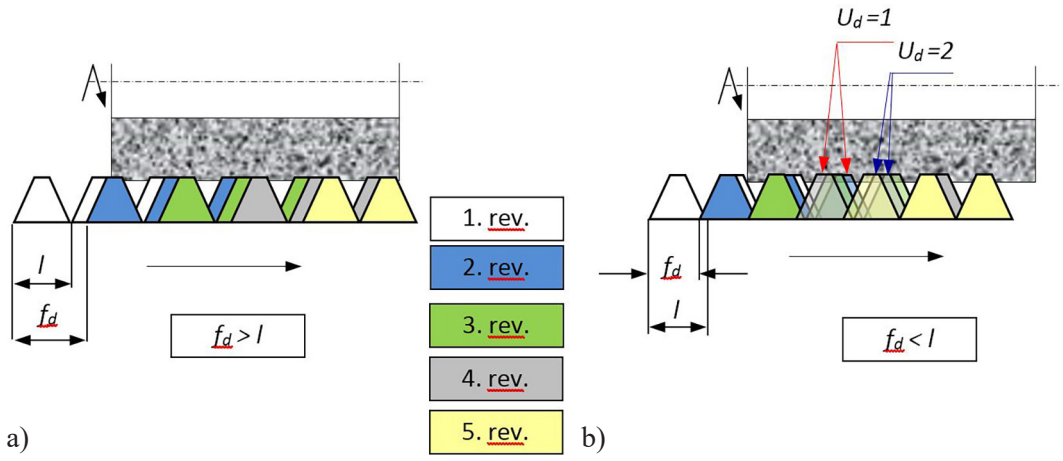

Figure 3. The position of the diamond tips of the stationary multi-grain dresser in relation to the grinding wheel generatrix in the next five revolutions of the grinding wheel: a) $f_d > l$; b) $f_d < l$; l – diamond distance, f_d – dressing feed [mm/rev]

position on the dresser surface and the parameters of the dressing process, and above all, the dressing feed f_d.

The above was the reason for performing a computer simulation in order to examine how the mentioned parameters affect the multiplicity of contact of the grinding wheel generatrix with diamonds. The variables of the simulation were: the number, active width and mutual position of diamond grits on the dresser surface, and the speed of dressing feed and the rotational speed of the grinding wheel. In the simulation, it was assumed that the diamond grits of the dresser are of the same size and their tops have the same active width. It was assumed that the cross-section of the diamond grits in the plane of the feed direction has the shape of an isosceles trapezoid with arms inclined to the base at an angle of 45°. The shorter base of the trapezoid represents the active width of the diamond. The simulation results were illustrated with graphs showing:

- distribution of traces of grains in the plane the grinding wheel generatrix,
- cross-sectional profile of the grinding wheel active surface,
- distribution of segments of the grinding wheel generatrix, on which the contact of the dresser diamonds with the surface of the grinding wheel occurred the same number of times.

Examples are shown in Figure 4. These are the results for two 6-grit dressers with different diamond settings. In the first one, one diamond grit is located centrally, and the other five are located at the corners of a regular pentagon. In the second, all diamonds occupy positions in the corners of a regular hexagon. In both cases, the outer diamonds are located on a circle with a diameter of 6 mm. The distribution of diamonds and their position in relation to the direction of grinding wheel movements are shown in Figures 4a and 4b. These drawings were supplemented with the value of the applied dressing feed f_d. In the simulation, it was assumed that the active width of the diamond tips is $b_d = 0.5$ mm.

A characteristic feature of the diamond traces distribution (Fig. 4 c, f) along the generatrix is the repetition of the same contact sequence over sections corresponding to the feed that the dresser performs during one wheel rotation. The

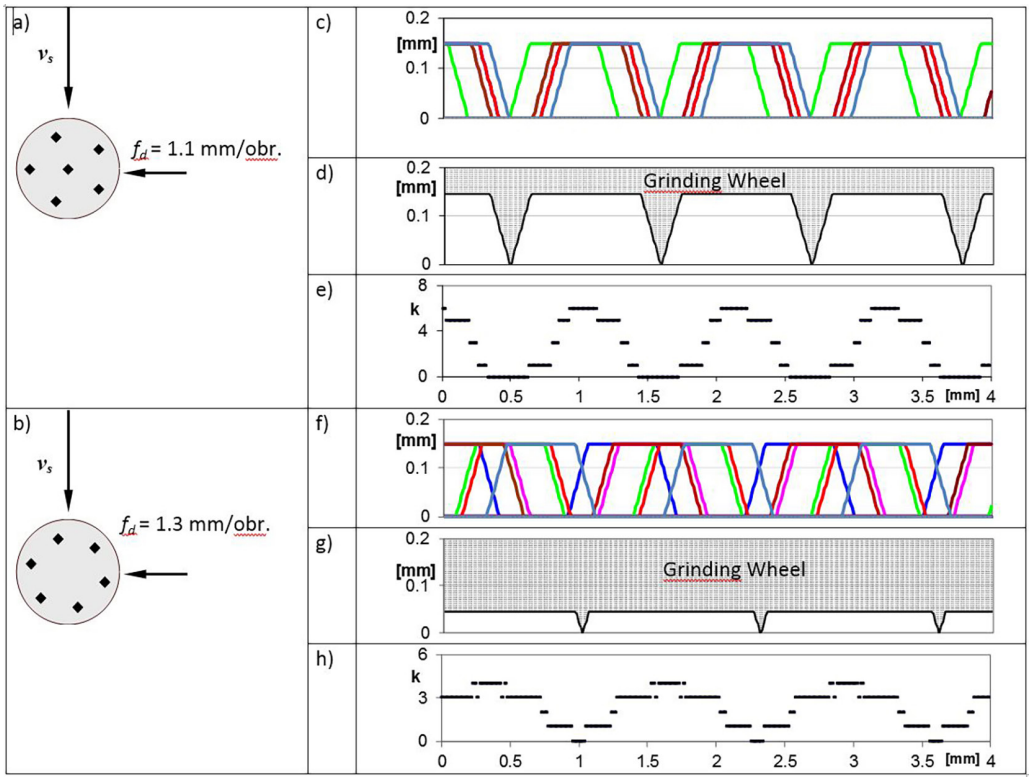

Figure 4. Examples of simulation results of the contact between diamonds grits of multi-point stationary dressers and the generatrix of a grinding wheel type 1: (a, b) setting the diamonds grits on the dresser surface, (c, f) grits traces distribution over the grinding wheel generatrix, (d, g) the profile of the grinding wheel generatrix, (e, h) overlap ratio along the generatrix of the grinding wheel

successive sections of generatrix are shaped by the dresser in the same way. The examples shown in Figure 4 illustrate situations in which the dressing parameters adopted did not ensure diamond contact along the entire length of the grinding wheel's generatrix during a single dressing pass. As a result, the generatrix took the shape of a comb with varying height and width of the teeth (Fig. 4 d, g). On the grinding wheel active surface formed in such conditions, there will be bands with multiple contact with the diamonds grits, which have been dressed with the overlap ratio U_d greater than 1, and the helical ridge. The change of the overlap ratio U_d along the grinding wheel generatrix during one dressing pass is shown in diagrams 4 e, h. The horizontal lines in the diagram represent the sections of generatrix on which the contact with the diamonds has repeated a certain number of times and the U_d ratio assumed the same value. The cited examples show that the effect that the multi-point dresser has on the grinding wheel active surface is differentiated along the generatrix and depends on the kinematic conditions of the process (dressing feed, grinding wheel rotational speed) and the characteristics of the dresser (active width and the position of diamonds grits relative to each other).

The indicators of dressing process with stationary multi-point dressers

The variable value of the dressing ratio U_d, with which the microbands are formed on the grinding wheel active surface, limits the possibility of using this index to characterize the dressing process performed with a stationary multi-point dresser. Therefore, a different index formula was proposed, which would play a similar role as the U_d and q_d ratios and more adequately represent the state of the grinding wheel topography after dressing. Since, after the dressing process, there are bands of different roughness next to each other on the surface of the grinding wheel, it was proposed that the dressing procedure should be characterized by an index averaging the local (occurring on individual bands) overlap ratios U_d.

The simulation results presented in Figure 4 show that the sections of grinding wheel generatrix (and therefore also individual bands), on which the overlap ratio U_d has specific values, have different lengths. Therefore, it was assumed that the formula of the new indicator would be specified by the weighted mean of the local dressing overlap ratios U_d occurring along the length of the generatrix. The weights of local ratios U_d in the calculated mean are the lengths of the sections on which these ratios occur. The method of calculating the indicator is described in Equation 4.

$$k_1 = \frac{\sum U_{dli} \cdot l_i}{l_c} \tag{4}$$

where: k_1 – mean overlap ratio [–], U_{dli} – local dressing overlap ratio of one dressing pass [–], l_i – the section length of the generatrix dressed with the local dressing overlap ratios k_1 [mm], l_c – length of the grinding wheel generatrix [mm].

When analyzing the formula (4), it can be seen that the dressing indicator k_1 will not have a special value (e.g. < 1, as in the case of the U_d ratio – Equation 1, informing that under the assumed process conditions, a section of the generatrix will not contact the diamonds at all. As already mentioned, under such conditions, a helical ridge is formed on the grinding wheel surface. Its presence is unfavorable for the grinding process. Therefore, it was proposed to calculate an additional indicator according to formula (5), which in such a case has a value less than one.

$$k_2 = \frac{f_d - l_0}{f_d} \tag{5}$$

where: f_d – dressing feed [mm rev^{-1}], l_0 – the total length of the grinding wheel generatrix that is not in contact with diamonds, defined within the distance of the dresser displacement during one grinding wheel rotation [mm].

The value of the presented indicators depends on the values related to the construction and condition of the dresser and the dressing process. To determine their value, you need data on the number, position and active width of diamonds grits and the dressing feed. Characteristic waveforms of changes in the indexes values depending on the mentioned values, developed using a computer simulation, are shown in Figures 6 and 7. The calculations were carried out assuming that the distances between the diamonds grits in the dresser are: (a) the same – Figure 5a, (b) irregular – Figure 5b and assuming that the active width of the diamonds grits is the same. Figure 5b demonstrates how irregular diamonds grits spacing is defined. It was assumed that the distance between the grits in the feed direction f_d is derived

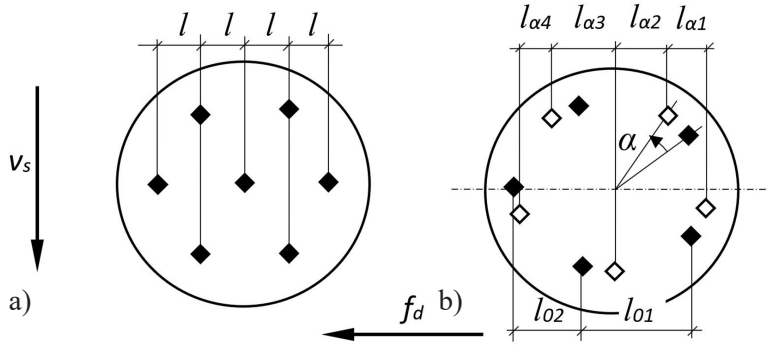

Figure 5. The diamonds arrangement on the dresser surface in relation to the direction of the dressing feed f_d: (a) distribution at equal intervals, (b) distribution at irregular intervals

from the setting of the dresser, in which the grits are located at the vertices of a regular polygon. If the dresser is rotated by the angle α, the distances between the polygon vertices (and therefore also the diamonds grits) measured in the feed direction f_d are not the same. The black quadrilaterals in Figure 5b show the grits in the starting position. The grit distances in such positioning are l_{01} and l_{02} respectively (it is a case of overlapping grit positioning in the direction of the grinding wheel speed v_s - hence there are only 2 distances). The non-blackened quadrilaterals show an example of the diamond grits positioning, when the dresser was rotated by the angle α in relation to the initial position. In this setting, successive grits are distant from each other by $l_{\alpha 1}$, $l_{\alpha 2}$, $l_{\alpha 3}$ and $l_{\alpha 4}$ and each of these values is not the same. Calculation for the angle α ranging from 0° to 360°/z (where z is the number of grits) is sufficient to determine all possible values that k_1 and k_2 will take for the described grits configuration on the dresser surface. Table 1 presents the ranges of variable values that were assumed in the calculations of k_1, k_2 indices.

Based on the performed calculations, graphs the values of k_1 and k_2 indicators as a function of grain distance l and dressing feed f_d were generated. Exemplary graphs are presented in Figures 6 and 7. These graphs, regardless of the adopted number of grains, have characteristic courses. Figure 6 applies to dressers with equal distances between diamonds determined by the value of l, while Figure 7 applies to the case when the distance between the diamonds in the direction of dressing feed is different and depends on the angle α which determines the angular position of the dresser. The analysis of the graph in Figure 6a shows that:

- the same mean overlap ratio values described by the k_1 indicator can be obtained by using dressers with a different diamonds grits spacing scale l , the value of the k_1 indicator is determined by the dressing feed f_d;
- the helical ridge on the surface of the grinding wheel is created when the dressing feed is a multiplicity of the distance between the diamonds in the dresser.

The graph in Figure 6b shows that with the increase of the feed rate, the mean value of overlap ratio (k_1) decreases and the density of points for which the k_2 indicator is less than 1 increases, which indicates the presence of areas not subjected to dressing on the surface of the grinding wheel. In the case of irregular diamond spacing in the dressing feed direction, the ranges of the α angle (defining the dresser position), for which a part of the grinding wheel will not be dressed, appear irregularly and have different widths (Fig. 7a). As the dressing feed rate increases, the ranges are larger and larger. When the lowest feed rates are applied, the k_1 indicator remains constant throughout the full range of the dresser settings.

Table 1. Variable value ranges adopted in the k_1, k_2 calculations

Number of diamonds grits z	The effective width of a single diamond grit b_d [mm]	Diamonds grits distance [mm]		Dressing feed f_d [mm/ rev]
		Regular	Irregular	
5, 6, 7	0.3	0.5 ÷ 2 every 0.1	Results from the α angle of the dresser position	0.3 ÷ 2 every 0.1

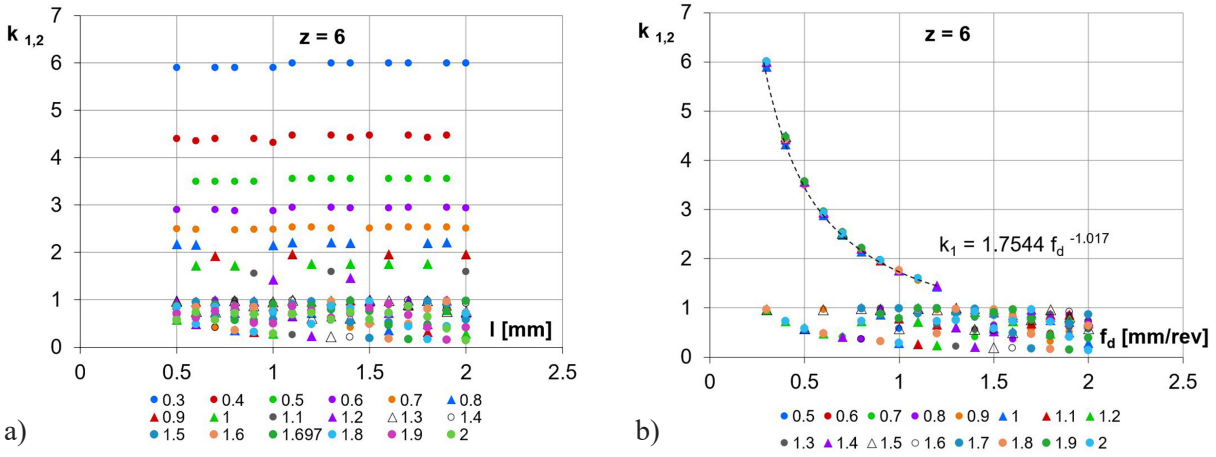

Figure 6. Stationary multi-point diamond dresser with equal distances between diamonds – the dependence of the k_1, k_2 value on: (a) diamond distances l (for different dressing feed f_d), (b) dressing feed f_d (for different diamond distances l)

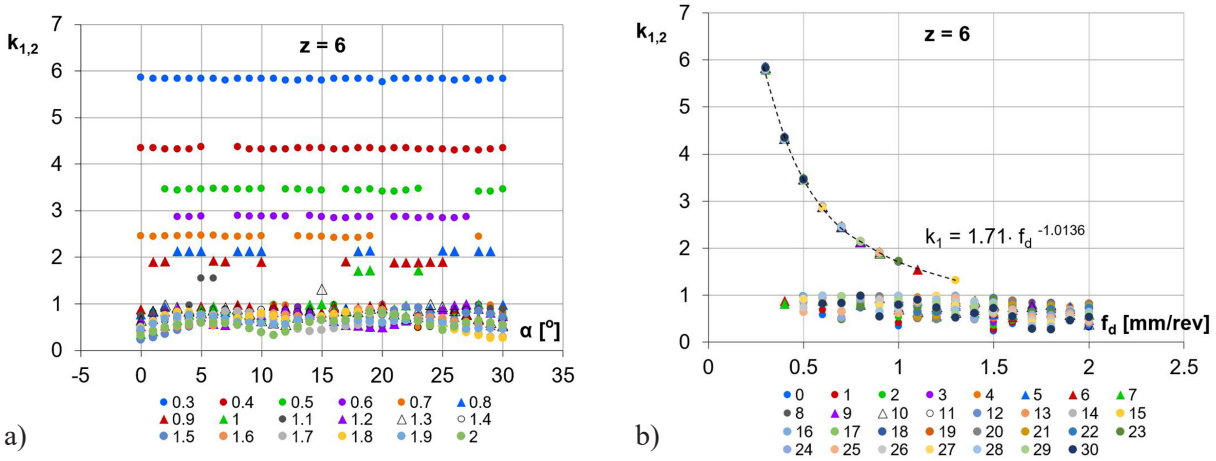

Figure 7. Stationary multi-point diamond dresser with irregular intervals between diamonds – the dependence of the k1, k2 value on: (a) the angle of the dresser positioning α (for different dressing feed fd); (b) dressing feed fd (for different angle α of the dresser positioning)

In both presented cases, the change in the value of the k_1 indicator in the feed rate function is not linear, but power – Figures 6b, 7b. This function proves that there is a decreasing influence of the increase of the dressing feed rate on the average value of the overlap ratio. The initial increase in the feed rate causes a rapid decrease in the indicator value, and then the effect weakens. These graphs indicate that there is a limit feed rate above which areas on the grinding wheel that are not in contact with the dresser diamonds cannot be avoided. The proposed k_1, k_2 indicators, which characterize the method of dressing with a multi-point diamond dresser, describe the obtained dressing effects in a similar way to the U_d ratio when applying single-point dressers. The analysis of the k_1 indicator values for various variants of diamonds distribution over the dresser active surface shows that, unlike the standard U_d ratio, they are not monotonic in the full range of the applied dressing feeds and there is no linear relationship between them. The k_1 indicator represents the average value of the overlap degree that was obtained on the grinding wheel generatrix during one dressing pass, on the basis of which it is possible to conclude about the achieved grinding wheel roughness. In turn, the k_2 indicator informs which combinations of dressing parameters should be avoided so that there are no areas on the grinding wheel surface that did not come into contact with the diamond grits of the dresser. The proposed indicators can therefore be a useful tool for forecasting the state of the topography of the grinding wheel active surface after dressing with a multi-point stationary dresser.

Topography of grinding wheel surface dressed with multi-point stationary diamond dresser

Since the surface of a grinding wheel dressed with a multi-point stationary diamond dresser consists of bands with varying microgeometry and active roughness, it is to be expected that the resulting functional properties of the grinding wheel are a superposition of the properties of individual bands. An attempt was made to assess the functional properties of the active grinding wheel surface based on the results of statistical analysis of microgeometry profiles of the wheel subjected to dressing operations characterized by different values of dressing indices k_1 and k_2.

Grinding wheel dressing conditions

The subject of the study was the active surface of aluminum oxide vitrified grinding wheel, which was dressed using various values of dressing indices $k_{1,2}$. A 6-grit dresser (WJA, Fig. 8) was used. Due to the hardness anisotropy of the diamonds, the grits were set in the same direction on the dresser's surface to ensure uniform wear resistance.

Figure 8. WJA 6-grit diamond dresser

The characteristics of the grinding wheel and the applied values of the dressing feed f_d are presented in Table 2. The grinding wheel was dressed on a SPG 30×80 surface grinder, equipped with a dressing feed control system. The dressing was performed with the use of coolant, without a spark-out passes.The holder with the dresser was placed on the electromagnetic table in a fixed position relative to the dressing feed direction (Fig. 9a). The adopted setting was maintained throughout the research period.

Consequently, the angle of diamonds orientation relative to the grinding wheel and the distances between diamonds measured in the dressing feed direction remained constant. Before the start of the main tests, the dresser was run-in - several dozen dressing passes of the grinding wheel, which was used in further tests, were made. Quantities necessary to calculate the dressing indices k_1 and k_2 , i.e. the active width of the diamond tips and their mutual distances, were measured on the dresser set in the working position, directly on the grinder. An optical microscope mounted on the grinding wheel guard (Fig. 9a) was used for observing the dresser's surface, the system for measuring the position of the grinder headstock was used to read the coordinates of the outlines of the diamond tops. The measurement consisted in reading the coordinates when the extreme points of the diamond tops touched the grid line of the microscope display screen (Fig. 9b). Due to the high resolution of the optoelectronic system for monitoring the grinder headstock position (1 μm), the measurement of the distance between the diamonds and their active width could be performed very precisely. Additionally, measuring directly on the grinder table avoided errors due to misalignment of the measurement direction with the feed direction, which might occur if measurements were taken on an external device. The high precision of the measurement was also ensured by the optical system of the microscope, which enabled the observation of the diamonds in the path of

Table 2. Dressing conditions

Grinding wheel	1 350 x 127 x 40 38A 46K VBE
Dresser	6- grit stationary (1carat)
Dressing parameters	a_d = 0.02 mm/2 x dressing pass (dressing finished without spark-out passes) f_d = (0.35; 0.6; 0.9; 1.2; 1.65) mm/rev with the use of coolant

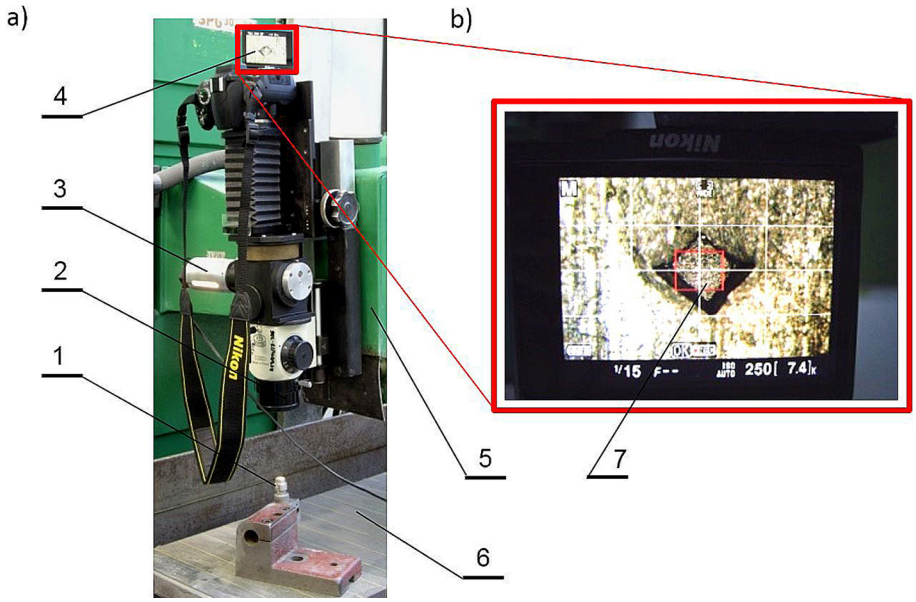

Figure 9. Optical microscope for the observation of dresser diamonds 1 – dresser, 2 – microscope lens, 3 – illuminator, 4 – display screen, 5 – grinding wheel guard, 6 – electromagnetic table, 7 – diamond tip

specular reflections. In this way, a high contrast was achieved between the top of the diamond and its remaining part (Fig. 9b), which allowed the precise outline of the top to be distinguished.

Based on the conducted measurements and the adopted range of feed rates, a chart of k_1, k_2 dressing indices values as a function of feed rate was developed (Fig. 10a). Figures 10c÷10g show what will be the distribution of local overlap ratios U_d along the grinding wheel generatrix for selected feed rate values. The discontinuity in the graph line in Figure 10a indicates that with a feed rate greater than approximately 1.55 mm/rev, during a single dressing pass on the grinding wheel generatrix, segments without contact with the diamond grits will occur. This means the possibility of a helical ridge forming on the grinding wheel surface. Smaller feed rates should ensure a mean overlap ratio k_1 ranging from 2 to 10.

Measurement method for grinding wheel surface topography

In order to determine the condition of abrasive grains and the position of their cutting edges on the grinding wheel surface, many methods are used. These methods, due to their capabilities and limitations, find applications in different research areas [17, 18]. Contact methods involving recording the changes in the height of the stylus

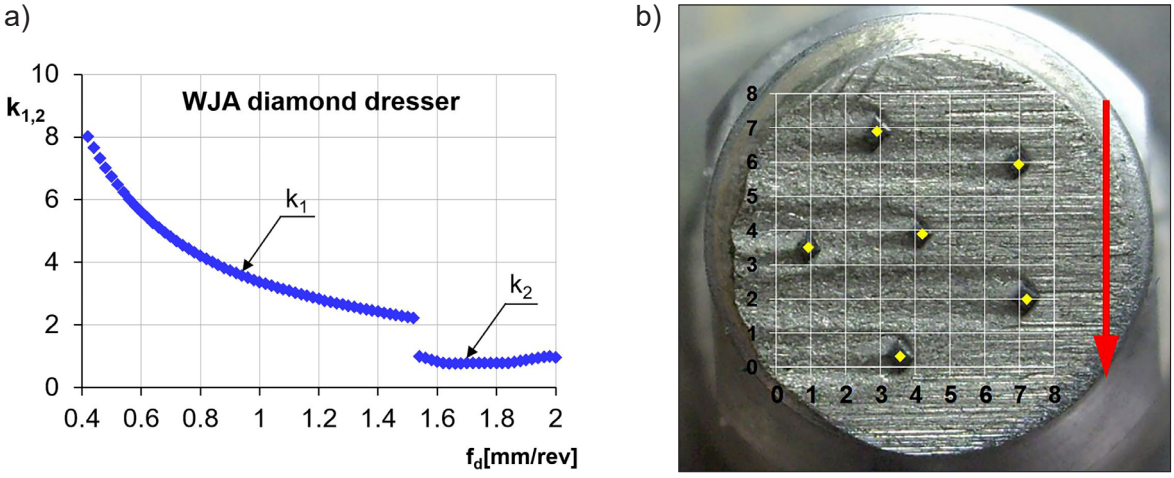

Figure 10. Dependence of k_1, k_2 indicators on dressing feed rate (WJA dresser)

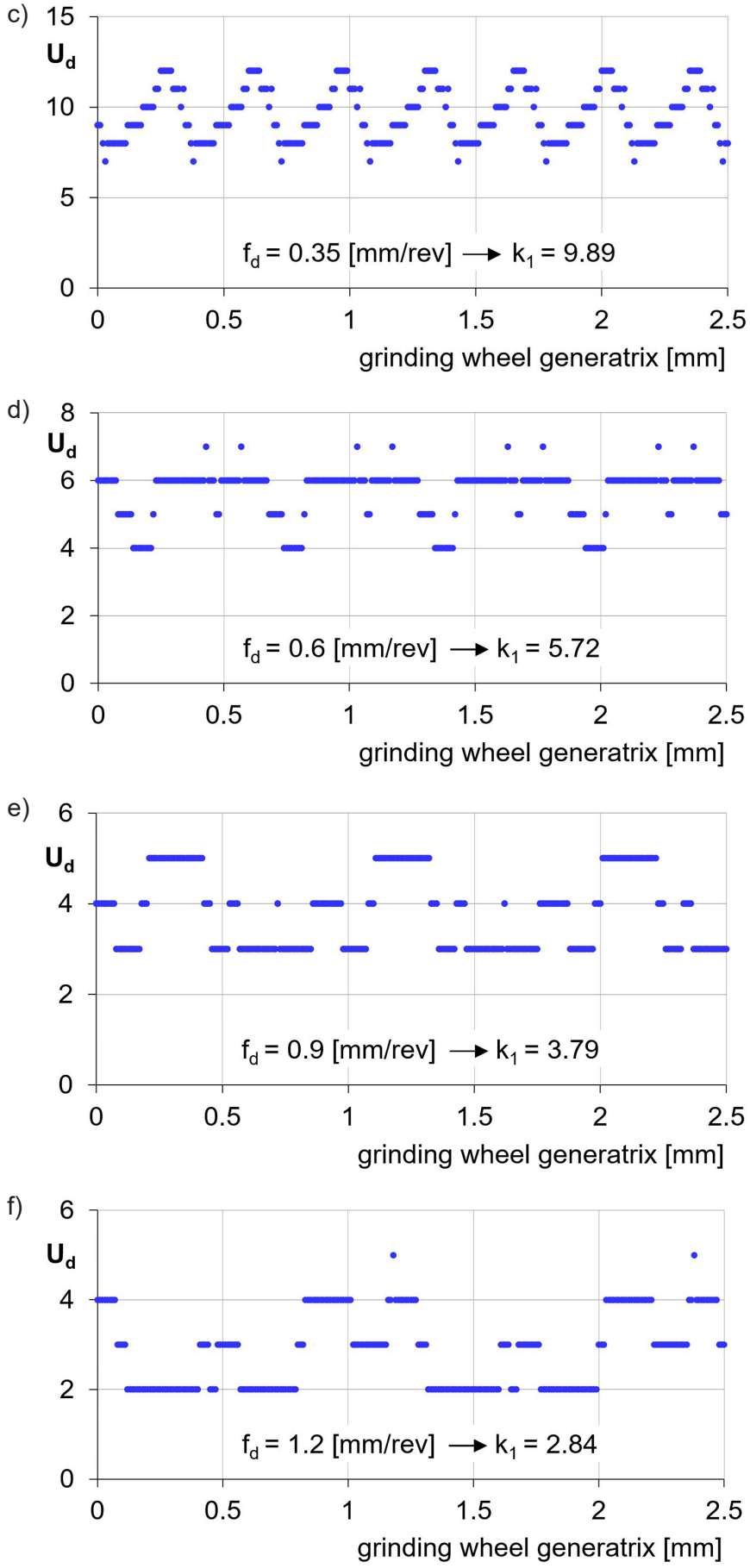

Figure 10. Cont. Dependence of k_1, k_2 indicators on dressing feed rate (WJA dresser)

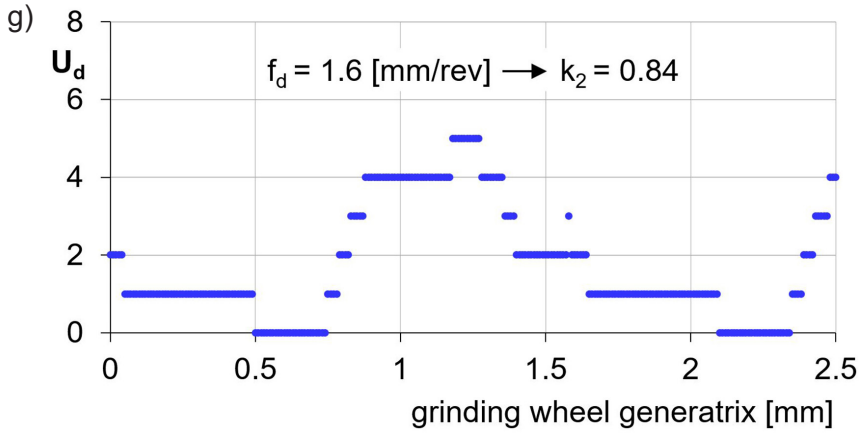

Figure 10. Cont. Dependence of k_1, k_2 indicators on dressing feed rate (WJA dresser)

sliding across the grinding wheel surface can be used to measure the 2D profile [9, 12, 13, 17, 19], as well as the 3D grinding wheel topography [11, 2021]. Such measurements are used for profile analysis [13, 19], modeling the grinding wheel topography [9] development of the new assessment parameters and measurement conditions [11, 21] assessment of changes in topography during the use of the grinding wheel [20], verification of the grinding wheel topography model after dressing [12]. Non-contact methods mainly rely on microscopic examinations where the recorded image comes directly from the grinding wheel surface or its replica. Optical microscopes [7, 15, 22], SEM [14, 23], laser confocal microscopes [24] and interference microscopes [25] are used in the research. A limitation of these methods is the restricted imaging area of the grinding wheel surface (typically only a few tens of mm²), which makes their application for quantitatively assessing the entire grinding wheel topography less practical. However, they remain invaluable for analyzing the state of abrasive grains. There are proposals for measurement strategies that use microscopic methods to measure the height of grains on a large surface of the grinding wheel. These strategies avoid the need for reconstructing the wheel's topography from a series of microscopic images, a process which is time-consuming and has limited accuracy [26]. However, this method is limited to determining a single parameter characterizing the grinding wheel's topography – the position of the grain apex relative to the grinding wheel's axis. It is applicable only to grinding wheels with defined grain positions (such as monolayer brazed grinding wheels). Fast measurement methods that are used during the operation of the grinding wheel on the grinder (e.g. laser displacement sensor [27]) have limited accuracy of mapping the grinding wheel microgeometry and can be useful for assessing significant changes in the topography that occur during the grinding wheel operation.

In the presented studies, the measurement of the grinding wheel topography was made using the contact method on a special stand with a slow-speed, aerostatically bearing spindle (Fig. 11). The rotational speed of the spindle ensured the peripheral speed of the grinding wheel, which was characteristic for the methods of contact assessment of surface roughness (i.e. 1 mm/s). The measurement unit of the ME10 profilometer was employed on the experimental setup. The analog signal from the ME10 amplifier was digitized by sampling it at a frequency corresponding to a displacement of the grinding wheel surface by 5 μm.

The method of evaluating the grinding wheel surface profile

The profiles obtained from the measurements were used to determine the statistical parameters of the distribution of cutting edges on the grinding wheel surface. In order to extract and determine the position of the active cutting edges, a computer simulation was conducted to model the penetration of the workpiece material into the working space of the grinding wheel surface. Figure 12 shows a fragment of the measured profile of the grinding wheel and the enlarged tip of the abrasive grain, with marked lines and the angle of material penetration. Since the depth of penetration of the workpiece into the surface of the grinding wheel is from a few to several micrometers [9, 19], a high level of signal amplification was used in the measurements. In this way, high

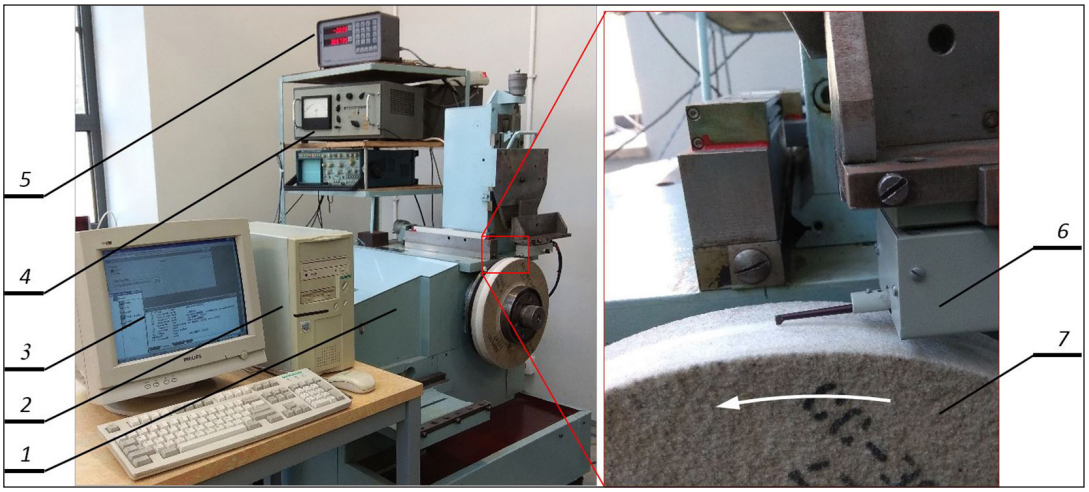

Figure 11. Experimental setup for measurement the circumferential profile of the grinding wheel surface: 1 – headstock, 2 – a computer with the AC card, 3 – TestPoint window, 4 – measuring amplifier ME10, 5 – grinding wheel position reader, 6 – measuring head ME10, 7 – grinding wheel

accuracy of mapping the part of the profile that is involved in the machining of the workpiece was obtained. However, this limited the measurement range, which did not cover the full depth of the profile. Hence, the lower part of the profile is not visible in Figure 12.

In the simulation, it was assumed that the grinding wheel surface is non-deformable. The angle of material penetration ε into the working space of the grinding wheel depends on the grinding parameters, and its average value is determined from equation (6) [9, 13, 19].

$$tg\varepsilon = 2\frac{v_{ft}}{v_s}\sqrt{\frac{a_e}{D_{eq}}} \tag{6}$$

where: v_{ft} – workpiece speed [m/s], v_s – grinding wheel speed [m/s], a_e – grinding feed [mm], D_{eq} – equivalent diameter of the grinding wheel [mm].

By employing the described simulation, the number and distribution of active cutting edges, as well as the undeformed chips thickness were determined.

Statistical assessment of the grinding wheel topography after dressing

After each dressing operation, three circumferential profiles of the grinding wheel surface were recorded. The measurements were taken in randomly selected areas along an arc of length 328 mm. The simulation of the penetration of the workpiece material into the working space of the grinding wheel was carried out assuming that the angle of penetration ε would correspond to conditions of medium-precise grinding, for which the value specified by equation (6) is 0.0002.

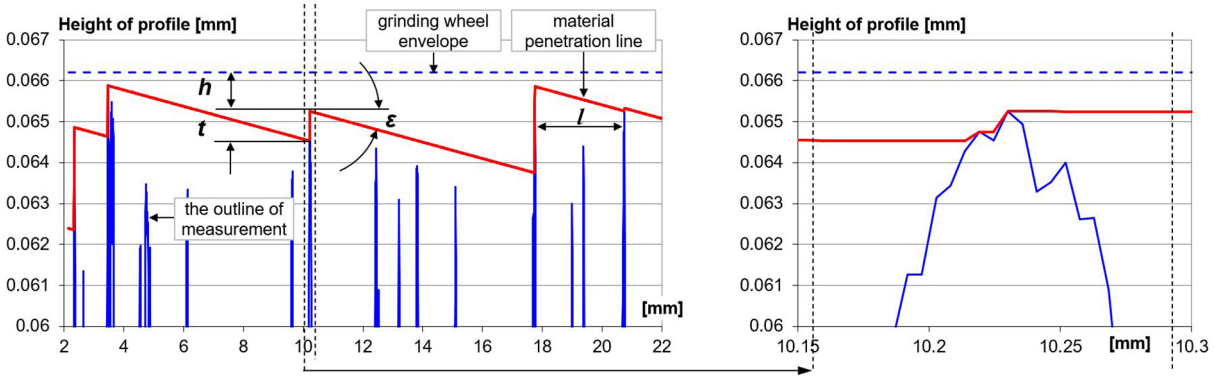

Figure 12. Simulation of the penetration of the workpiece material into the working space of the grinding wheel ε – average angle penetration, t – undeformed chip thickness, h – depth of active cutting edges, l – distance between active cutting edges

The graphs in Figures 13÷16 show the statistical elaboration of the simulation results. The notations used in the graphs consist of a component representing the applied dressing feed rate and another component indicating the measurement number of the grinding wheel topography.

The two-sample Kolmogorov-Smirnov test was employed to check whether two samples of undeformed chip thickness or depths of active cutting edges, derived from measurements conducted after dressing the grinding wheel with a specified dressing feed rate, came from the same distribution. A negative test result could indicate that the grinding wheel topography measured along different arcs of the grinding wheel circumference is not the same. Conducting the test involved verifying whether the cumulative distribution functions determined within the results obtained for a specific dressing feed rate f_d differed from one another. Calculations were performed for each pair from the three determined functions. The profiles of the cumulative distribution functions, which are characteristic for almost all conducted simulations, are shown in Figure 13. The graphs of the cumulative distribution function for chip thickness have (Fig. 13a) similar profiles, while in the case of the active cutting edge depth function (Fig. 13b), one of the graphs significantly deviates from the others.

Table 3 presents the results of calculations of the λ-statistic of the Kolmogorov-Smirnov test. It is generally considered that two distributions differ from each other if, for the adopted level of significance, the statistic λ exceeds the critical value. In the conducted research, it was assumed that the significance level is 0.05, which corresponds to the value of the λ_{kr} = 1.36 statistics. Table cells with results exceeding the indicated value are marked with a colored background. The calculations confirmed earlier observations – only in the case of dressing feed of 1.2 mm/rev the test showed that all measurements represent the same distribution. In the other cases of the applied dressing feeds, one of the measurements significantly differs from the others - the value of the statistics significantly exceeds the critical value, which indicates that the microgeometry of this arc differs from the others - the probability of cutting edges at a different depth increases.

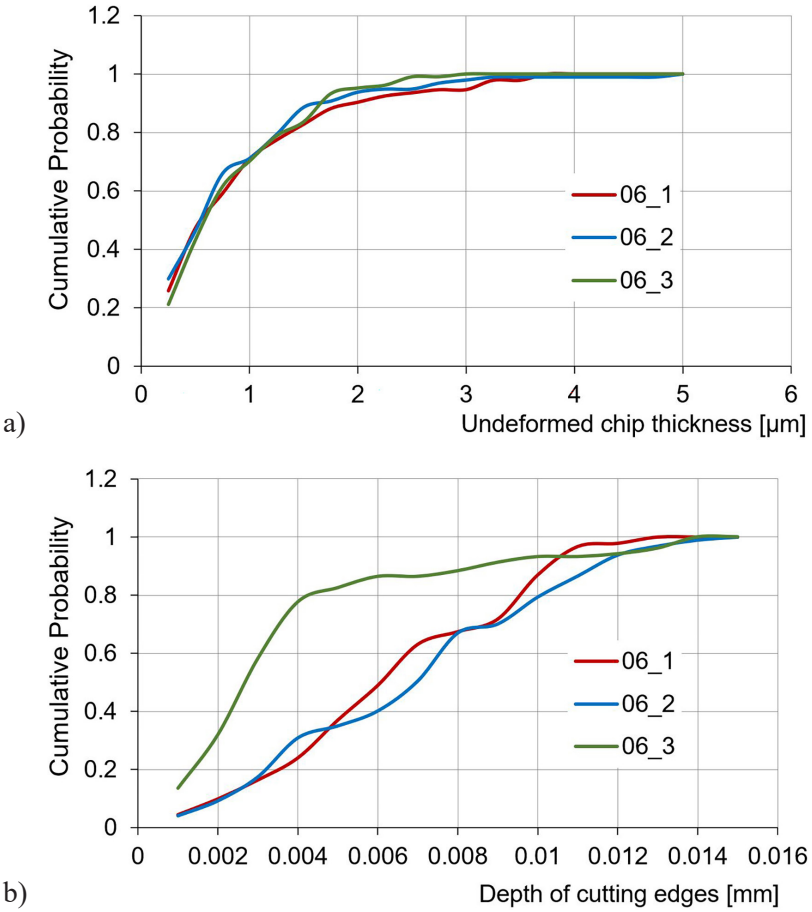

Figure 13. Cumulative distribution functions of the undeformed chip thickness (a) and depth of cutting edges (b)

Table 3. The value of the statistic λ of two-sample Kolmogorov-Smirnov test

Compared distributions	f035 1-2	f035 1-3	f035 2-3	f06 1-2	f06 1-3	f06 2-3	f09 1-2	f09 1-3	f09 2-3	f12 1-2	f12 1-3	f12 2-3	f16 1-2	f16 1-3	f16 2-3
Undeformed chip thickness	0.38	0.79	0.77	0.47	0.39	0.62	1.18	0.40	1.15	0.80	0.59	0.59	0.42	0.47	0.46
Depth of cutting edges	1.29	3.74	3.66	0.86	3.75	3.36	1.72	1.73	1.10	0.89	1.14	1.00	3.79	3.27	0.69

For the case presented in Figure 13, in the area of the grinding wheel where measurement 06_3 was made, the probability of the occurrence of edges at smaller depths is higher. This might result from the dresser's operation method in this area of the grinding wheel – there was an intense overlapping of the dresser's diamonds work paths, leading to dressing with a high overlap ratio as a consequence. The similarity of the undeformed chips thickness distributions may be the result of extracting many cutting edges on individual abrasive grains during the simulation. The white aluminum oxide used in the construction of the grinding wheel has a tendency to micro-fracturing, which causes the grain tips to be jagged, and the resulting cutting edges are able to cut chips of small thickness. Their large number extracted during the simulation homogenizes the course of all the cumulative distribution functions. A collective summary depicting the location, shape, and distribution of the sets of the depth of cutting edges and undeformed chips is presented in the box plots shown in Figures 14 and 15. These are median/quartile/minimum, maximum type plots, which are characterized by the following values:

- Me – median (middle value of the data set),
- Q1 – first quartile (25% of all results),
- Q3 – third quartile (75% of all results),
- IQR – interquartile range,
- IQR = (Q3 - Q1) – box length,
- Q1 – 1.5 · IQR ≥ outliers ≥ Q3 + 1.5 · IQR
- Q1 – 3 · IQR ≥ extreme values ≥ Q3 + 3 · IQR

Displayed in Figure 16, the last of the statistical description plots of circumferential grinding wheel surface profiles, illustrates the change in the total count of active cutting edges as a function of the applied dressing feed rate.

Based on the results of statistical analysis, shaping of the grinding wheel topography with the multi-point diamond dresser using a specific dressing feed can be described as follows:

- f_d = 0.35 mm/rev – in relation to other cases, the effect of using the smallest dressing feed is to obtain the largest number of active edges (Fig. 16), which are concentrated at the smallest depth of the CPS profile (Fig. 14). The chips generated during grinding with a grinding wheel dressed in this way will be very fine (Fig. 15).
- f_d = 0.6 mm/rev – the result of the action of the dressing tool moving at a slightly higher

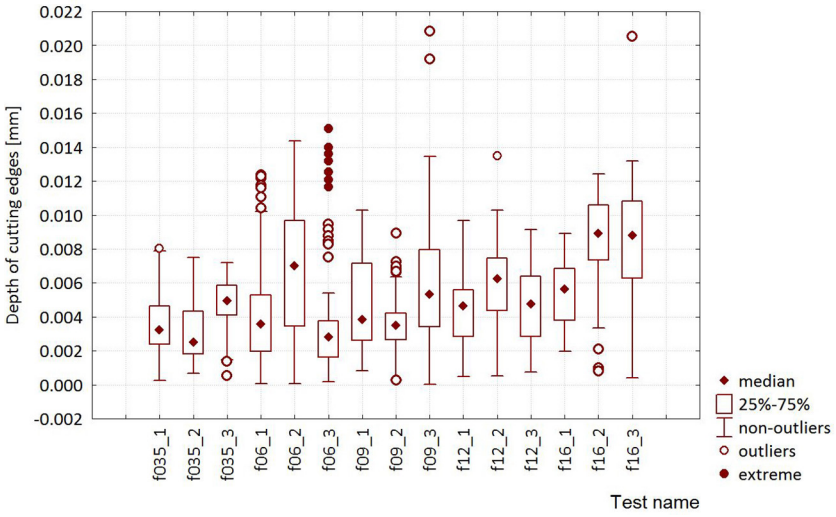

Figure 14. Boxplot of the depth of cutting edges

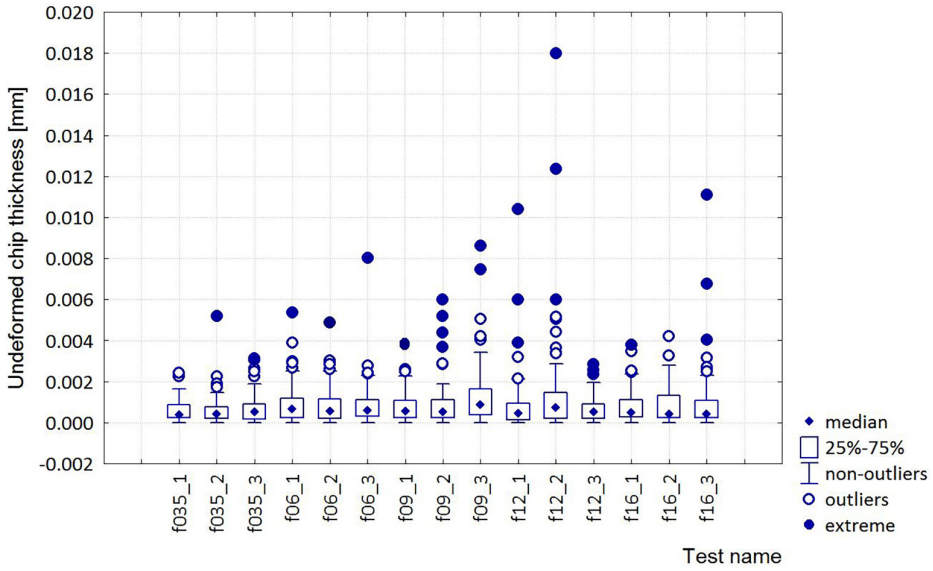

Figure 15. Boxplot of undeformed chip thickness

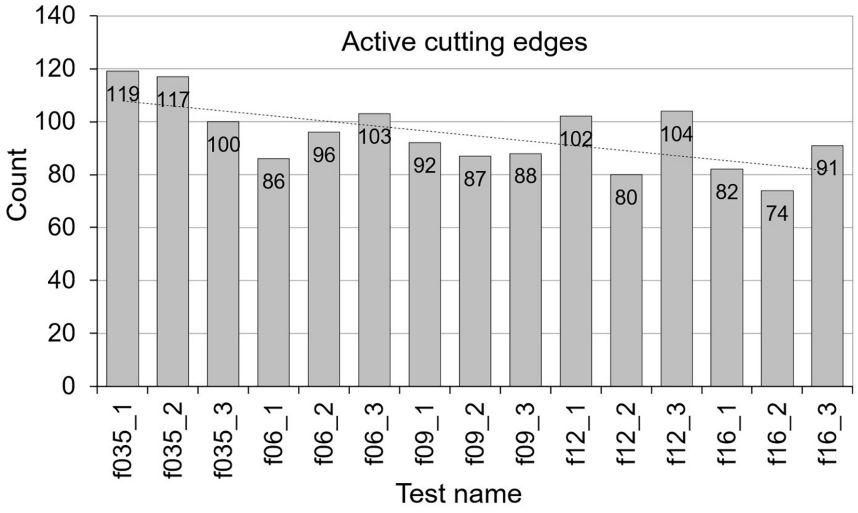

Figure 16. The count of active cutting edges on the grinding wheel surface after dressing with the WJA dresser at different dressing feed rates

feed rate is the formation of a smaller number of active cutting edges with greater dispersion at the depth of the grinding wheel surface profile. The distribution of cutting edges ensures a similar, apart from three extreme values, thickness of the cut layer in all analyzed measurement areas. The edges are similarly loaded, because the thickness of the cut layer changes in a small range.

- f_d = 0.9 mm/rev – increasing the dressing feed rate to 0.9 mm/rev resulted in a further reduction in the number of active cutting edges compared to previous cases, but to a slight extent, it affected the increase in their dispersion at different depths of the grinding wheel surface. However, it increased the thickness of undeformed chips formed during grinding.
- f_d = 1.2 mm/rev – depending on the place of measurement of the grinding wheel surface, there was a significant difference in the number of active cutting edges. When their number in the sample reached the highest values (Fig. 16: f12_1 and f12_3), the undeformed chip thickness is small, and the edges occur at a smaller depth of the profile. The smaller number of edges determined in the f12_2 measurement is distributed over a greater depth of the profile, due to which the thickness of the undeformed chips reaches extreme values (Fig. 15).

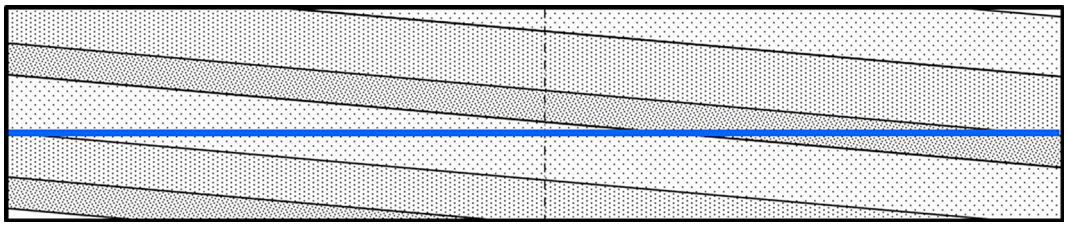

Figure 17. Trace of the measurement line of the grinding wheel surface against the background of bands formed with local overlap ratios U_d

- f_d = 1.6 mm/rev – dressing with the highest applied feed rate results in the smallest number of cutting edges distributed at the greatest depth of the profile in relation to the other cases (Fig. 14). The undeformed chip thickness is similar in the three analyzed measurements.

The provided descriptions average the obtained results, indicating the overall trend of changes in the grinding wheel's topography due to the application of different dressing feed rates. However, the general conclusion arising from the Kolmogorov-Smirnov test and the boxplots, especially regarding the distribution of active cutting edges, is the creation of diverse topography on the grinding wheel surface when using specific dressing feed rate. The reasons for the formation of such topography should be sought in the formation of helix bands on the surface of the grinding wheel (with a pitch equal to the feed of the dresser per one revolution of the grinding wheel), where the U_d ratio assumed different values – as shown in Figure 10. The profilometer stylus intersecting these bands (Fig. 17, blue color) recorded profiles characteristic of local overlap ratios. Since the selection of measurement areas was random and the length of the measurement arc constituted about 0.3 of the grinding wheel circumference, the measurement result depended on the width of individual bands and their contribution to the profile reproduced by the profilometer stylus. The change in topography when using high feed rates also results from the change in dressing depth that occurs when removing the spiral ridge left over from the previous dressing pass.

CONCLUSIONS

The results of the conducted research allow for the presentation of the following conclusions: k_1 and k_2 indices are useful for monitoring the dressing of grinding wheels with the use of stationary multi-point dressers. The k_1 index represents the average value of the overlap ratio that was obtained on the grinding wheel generatrix during one dressing pass, on the basis of which it is possible to conclude about the achieved grinding wheel roughness. The k_2 index informs which combinations of dressing parameters should be avoided so that there are no areas on the grinding wheel surface that did not come into contact with the diamond grits of the dresser.

The surface of the grinding wheel dressed with a stationary multi-point dresser, without spark-out passes, shows zone-differentiated microgeometry. Hence, dressing using multi-point stationary diamond dressers can be recommended only for rough machining operations. In order to achieve a consistent microgeometry across the entire grinding wheel surface, dressing with a stationary multi-point diamond dresser should be conducted using small dressing feeds or performing spark-out passes. In both cases, the resulting active surface roughness of the grinding wheel will be low, rendering it unsuitable for efficient grinding operations.

During the initial usage of newly acquired dressers with sharp diamond tips, characterized by a small active width, there is an increased risk of forming a spiral ridge on the grinding wheel surface. To prevent this undesired outcome of dressing, it is important to appropriately select the dressing feed using the k_2 indicator.

REFERENCES

1. Tawakoli T., Abdolreza Rasifard A. Dressing of Grinding Wheels. In Machining with Abrasives, Jackson, M.J., Davim, J.P., Eds.; Publisher: Springer Science+Business Media 2011. 181–243. doi. org/10.1007/978-1-4419-7302-3_4
2. WINTER diamond tools for dressing grinding wheels, Catalogue No. 5
3. Wegener K., Hoffmeister H.W., Karpuschewski B. Kuster F., Hahmann W.C., Rabiey M. Conditioning

and monitoring of grinding wheels. CIRP Annals - Manufacturing Technology. 2011; 60: 757–777. doi:10.1016/j.cirp.2011.05.003

4. Brinksmeier E., Cinar M. Characterisation of dressing processes by determination of collision number of the abrasive grits. Ann. CIRP. 1995; 1: 299–304.
5. Azizi A., Rahimi A., Rezaei S.M., Baseri H. Modeling of dressing forces during rotary diamond cup dressing of vitrified CBN grinding wheels. Mach. Sci. Technol. 2009; 13: 407–426. doi.org/10.1080/10910340903237822
6. Linke B. Dressing process model for vitrified bonded grinding wheels. CIRP Ann. - Manuf. Technol. 2008; 57: 345–348. doi.org/10.1016/j.cirp.2008.03.083
7. Palmer J., Ghadbeigi H., Novovic D., Curtis D. An experimental study of the effects of dressing parameters on the topography of grinding wheels during roller dressing. J. Manuf. Process. 2018; 31: 348–355. doi.org/10.1016/j.jmapro.2017.11.025.
8. Aleksandrova I. Optimization of the Dressing Parameters in Cylindrical Grinding Based on a Generalized Utility Function. Chinese Journal of Mechanical Engineering 2016; 29: 63–73. doi.org/ 10.3901/CJME.2015.1103.130.
9. Urbaniak M. Cutting properties evaluation system of vitrified grinding wheels. Scientific Bulletin of Lodz Technical University. 2002; 913.
10. König W., Messer J. Beeinflussung von Topographie und Prozessverhalten keramisch gebundener Schleifscheiben durch die Abrichtbedigungen. Industrie Diamanten Rundschau 1981, 2.
11. Blunt L., Ebdon S. The application of three-dimensional surface measurement techniques to characterizing grinding wheel topography. Int. J. Machine Tools Manuf. 1996; 36(11): 1207–1226. doi.org/10.1016/0890-6955(96)00041-7.
12. Torrance A.A., Badger J.A. The relation between the traverse dressing of vitrified grinding wheels and their performance. Int. J. of Machine Tools & Manufacture. 2000; 40: 1787–1811. doi.org/10.1016/S0890-6955(00)00015-8.
13. Verkerk J. Final report concerning CIRP cooperative work on the characterization of grinding wheel topography. Ann. CIRP. 1977; 26(2): 385–395.
14. Li M., Ding W., Li B., Xu J. Morphological evolution and grinding performance of vitrified bonded microcrystal alumina abrasive wheel dressed with a single-grit diamond. Ceramics International. 2019; 45: 19669–19678. doi.org/10.1016/j.ceramint.2019.06.216.
15. Haoyang Cao, Xun Chen, Haolin Li: Dressing strategy and grinding control for cylindrical microstructural surface. The International Journal of Advanced Manufacturing Technology. 2018; 99: 707–727.
16. Sheiko M.N., Maksimenko A.P. Dressing with Diamond Sticks from the Standpoint of Mechanical-Statistical Concepts of Diamond Abrasive Machining. Steady-State Actual Infeed in the Multiple-Pass Mode. Journal of Superhard Materials. 2008; 30(4): 282–286.
17. Cai R., Rowe W.B., Morgan M.N., Mills B. Measurement of vitrified CBN grinding wheel topography. Key Eng. Mater. 2003; 238–239: 301–306.
18. Boaron A., Weingaertner W.L. Dynamic in-process characterization method based on acoustic emission for topographic assessment of conventional grinding wheels. Wear. 2018; 406–407: 218–229.
19. König W., Lortz W. Properties of cutting edges related to chip formation in grinding. Annals of the CIRP 1975; 24(1): 231–235.
20. Butler D.L., Blunt L.A., See B.K., Webster J.A., Stout K.J. The characterisation of grinding wheels using 3D surface measurement techniques. J. Mater. Process. Technol. 2002: 127(2): 234–237.
21. Nguyen A.T., Butler D.L. Correlation of grinding wheel topography and grinding performance: a study from a viewpoint of three dimensional surface characterization. J. Mater. Process Technol. 2008; 208: 14–23.
22. Kapłonek W., Nadolny K., Królczyk G.M. The use of focus-variation microscopy for the assessment of active surfaces of a new generation of coated abrasive tools. Measurement Science Review. 2016; 16: 42–53.
23. Huang H. Effects of truing/dressing intensity on truing/dressing efficiency and grinding performance of vitrified diamond wheels. J. Mater. Process. Technol. 2001; 117: 9–14.
24. Zhang Y.Z., Fang C.F., Huang G.Q., Xu X.P. Modeling and simulation of the distribution of undeformed chip thicknesses in surface grinding. Int. J. Mach. Tools Manuf. 2018; 127: 14–27. doi.org/10.1016/j.ijmachtools.2018.01.002.
25. Lefebvre A., Sinot O., Torrance A. Optimization of dressing conditions for a resin-bonded diamond wheel by topography analysis. Machining Science and Technology. 2013; 17: 312–324.
26. Chen J., Cui C., Huang G., Huang H., Xu X. A new strategy for measuring the grain height uniformity of a grinding wheel. Measurement. 2020; 151: 107250. doi.org/10.1016/j.measurement.2019.107250.
27. Kim S.H., Ahn J.H. Decision of dressing interval and depth by the direct measurement of the grinding wheel surface. J. Mater. Process. Technol. 1999; 88: 190–194.
28. Klocke F. Zerspanung mit geometrisch unbestimmter Schneide. Vorlesung. Werkzeugmaschinenlabor WZL der RWTH Aachen. 2008; 54, 64.